

# Quantum coupled-channels model of nuclear fusion with a semiclassical consideration of neutron rearrangement

A. V. Karpov,<sup>\*</sup> V. A. Rachkov, and V. V. Samarin*Flerov Laboratory of Nuclear Reactions, JINR, 141980 Dubna, Russia*

(Received 31 August 2015; published 4 December 2015)

**Background:** Significant enhancement of sub-barrier fusion cross sections owing to neutron transfer with positive  $Q$  values was observed in many combinations of colliding nuclei. This degree of freedom has not yet been included into the rigorous quantum coupled-channels (QCC) approach. However, the empirical coupled-channels model with neutron rearrangement [Zagrebaev, *Phys. Rev. C* **67**, 061601 (2003)] has already been successfully used in several papers to reproduce and predict cross sections for sub-barrier fusion reactions of stable nuclei.

**Purpose:** The objective of this study is to combine the QCC approach and the empirical model to account for additional channels of neutron rearrangement.

**Method:** Coupling of relative motion to collective degrees of freedom (rotation of nuclei and/or their surface vibrations) are taken into account within the QCC approach. The probability of transfer of  $x$  neutrons with a given  $Q$  value is estimated semiclassically.

**Results:** The proposed new model was successfully tested on a few combinations of fusing nuclei  $^{40}\text{Ca} + ^{90,94,96}\text{Zr}$ ,  $^{32}\text{S} + ^{90,94,96}\text{Zr}$ , and  $^{60,64}\text{Ni} + ^{100}\text{Mo}$ . The calculated fusion cross sections and barrier distribution functions agree well with experimental data.

**Conclusions:** The model developed in this work confirms all the conclusions previously made within the empirical coupled-channels model with neutron rearrangement [see Rachkov *et al.*, *Phys. Rev. C* **90**, 014614 (2014)]. Moreover, it has an advantage of a more reliable microscopic account for the coupling between relative motion and the collective degrees of freedom. The proposed model can also be used to reproduce the structure of the barrier distribution function. This is a step forward to a complete solution of the long-term problem of accounting for neutron transfer channels in the QCC model.

DOI: [10.1103/PhysRevC.92.064603](https://doi.org/10.1103/PhysRevC.92.064603)

PACS number(s): 25.70.Jj, 25.70.Hi, 24.10.Eq

## I. MOTIVATION

The process of nuclear fusion remains one of the most intriguing and intensively studied phenomena, both theoretically and experimentally. The study of this process is very important, for example, for synthesis of superheavy nuclei and understanding of astrophysical nucleogenesis; it casts additional light on the influence of different inelastic excitations and/or breakup channels on the fusion cross section, etc. Over the past decades, experimental sensitivity has been tremendously improved, and the intensities of radioactive beams were increased. This allowed, in particular, systematic investigations of fusion of stable as well as exotic nuclei at energies well below the Coulomb barrier. An interesting and rather exiting phenomenon was found for some combinations of fusing nuclei. Coupling of relative motion to other collective degrees of freedom, such as the rotation of deformed nuclei and their surface vibrations, is commonly thought to be the main cause of strong enhancement of sub-barrier fusion. However, a considerable body of experimental data reveals that additional enhancement of the sub-barrier fusion cross section is due to neutron rearrangement with positive  $Q$  values. This effect can be easier observed if one compares sub-barrier fusion cross sections for two close projectile-target combinations. One of them allows neutron rearrangement with positive  $Q$  values, whereas neutron transfer for another combination

goes with negative  $Q$  values. The combinations ( $^{40}\text{Ca} + ^{96}\text{Zr}$ ,  $^{40}\text{Ca} + ^{90}\text{Zr}$ ) [1] and ( $^{16}\text{O} + ^{60}\text{Ni}$ ,  $^{18}\text{O} + ^{58}\text{Ni}$ ) [2] are good examples of such kind. Coupling of relative motion to surface vibrations of colliding nuclei describes quite well the fusion cross sections for the  $^{40}\text{Ca} + ^{90}\text{Zr}$  and  $^{16}\text{O} + ^{60}\text{Ni}$  reactions, but it is insufficient to describe additional sub-barrier fusion enhancement for the  $^{40}\text{Ca} + ^{96}\text{Zr}$  and  $^{18}\text{O} + ^{58}\text{Ni}$  reactions (see, e.g., Refs. [3,4] for detailed discussion).

The nucleon transfer in low-energy nucleus-nucleus collisions can be described theoretically within the models based on the first-order perturbation theory such as GRAZING [5] and complex Wentzel-Kramers-Brillouin approximation [6]; in the framework of the time-dependent Hartree-Fock (TDHF) theory (see Refs. [7–9] and references therein); within the models based on the time-dependent Schrödinger equation [10–12]; as well as in the dynamical approaches employing the Langevin-type equations [13,14]. The whole dynamics of the near-barrier fusion can be considered microscopically in the TDHF theory [7,9]. At the same time, rearrangement of a few valence neutrons only may significantly influence the sub-barrier fusion probability. In this case, the semiclassical approach used in this work can be a good approximation to the fully microscopical treatment (see below).

The influence of the coupling to neutron transfer channels on the sub-barrier fusion probability can be explained in the following way [3]. At the approaching reaction stage the valence neutron's wave function, localized initially in one of the nuclei, may spread into the volume of the other nucleus (see, e.g., Refs. [7,9,11,12]) already *before* the colliding nuclei

<sup>\*</sup>karpov@jinr.ru

have overcome the Coulomb barrier. This process may go with the energy profit which, in turn, may lead to a gain in the kinetic energy of relative motion (energy lift). Thus, neutron transfer (rearrangement) with positive  $Q$  values may significantly influence the sub-barrier fusion dynamics, giving a substantial increase of the barrier penetration probability.

Even a more pronounced effect of neutron rearrangement was observed experimentally (see Refs. [15–23]) for the reactions with neutron-rich weakly bound nuclei, such as  ${}^6\text{He}$ , with stable targets. The coupling to surface vibrations and to rotation of heavy target in these cases are less important because of a smaller size of the projectile. However, rearrangement of neutrons at the approaching stage can lead to a noticeable enhancement of sub-barrier fusion owing to large positive  $Q$  values. Deep sub-barrier fusion of light nuclei (including the exotic ones) can also be important for astrophysical nucleosynthesis [11].

The cross sections of near-barrier fusion of nuclei and, in particular, the sub-barrier fusion enhancement induced by surface deformations or rotations of heavy deformed nuclei can be properly described within the quantum coupled-channels (QCC) model [24–29] or within the empirical coupled-channels (ECC) model [30]. On the other hand, it is rather difficult to include nucleon transfer channels in the rigorous QCC approach. The problem occurs when, following the standard coupled-channels method, the total wave function is decomposed both over the collective (rotational and/or vibrational) states and neutron transfer states. In such a decomposition overcomplete and nonorthogonal basis functions are used that require complicated technique or certain simplifying assumptions.

One of the first attempts to account for neutron rearrangement within the coupled-channels approach is made in Ref. [25] where the well-known CCFULL code is described. This is done by adding a phenomenological term responsible for neutron transfers to the total Hamiltonian. It is assumed that this term has the form factor similar to the one corresponding to the vibrational mode. An adjustable coupling constant is fitted to experimental data.

A series of works devoted to this problem was published by Sargsyan and others (see, e.g., Refs. [31,32]). The approach is based on the assumption that at the approaching stage of the fusion process the neutron pair transfer can occur with a certain probability, leading to a change in nucleon composition of fusing nuclei. Thus a new pair of nuclei with different collective properties and, hence, with different enhancement of sub-barrier fusion can be formed.

In Refs. [12,33] an attempt to develop a fully microscopic CC approach taking account of neutron rearrangement was made. Following the idea of Refs. [34,35] the neutron rearrangement process is described basing on the decomposition of the neutron's wave functions over a set of two-center states in combination with the TDSE method. Neutron transitions to the two-center levels corresponding to different  $Q$  values and a possible decrease of the initial two-center level are considered. This may lead to a gain in the kinetic energy of relative motion and, hence, cause an additional enhancement of sub-barrier fusion. This approach is still under development. It is noteworthy that simplified assumptions are used. For

example, the two-center excitation spectrum is assumed to be a pure single-particle one; therefore, the transitions only between single-particle states are treated. Even with these simplifications, the computational scheme is still too complicated and time-consuming.

In Ref. [3] neutron rearrangement was quite consistently incorporated into the ECC approach using a semiclassical approximation for transfer probability. This method is not fully microscopic, but takes into account the main effects of neutron rearrangement with positive  $Q$  values. The ECC model with neutron rearrangement has already been successfully used in several papers [3,4,36–38] to reproduce and predict cross sections for the sub-barrier fusion reactions of stable nuclei. We have recently published a paper [4] devoted to the study of the influence of neutron rearrangement channels with positive  $Q$  values on sub-barrier fusion. The main conclusion of the paper is that a pronounced enhancement (visible above those caused by the coupling to the collective vibrational and/or rotational degrees of freedom) of sub-barrier fusion owing to neutron rearrangement can be expected, if the following necessary conditions are fulfilled: (i) large positive  $Q$  values are present for one- and/or two-neutron transfer, while the influence of the  $xn$  channels for  $x > 4$  is negligible; (ii) fusion enhancement owing to coupling to collective states is relatively small, like in the case of fusion of light nuclei and spherical magic or nearly magic nuclei. With regard to fusion of light nuclei, there is an additional condition requiring the neutron binding energies in the donor nucleus to be small (the classical example is the fusion of light weakly bound nuclei, like  ${}^6\text{He}$ ). Note that all the calculations in Ref. [4], as well as the QCC calculations without neutron transfer presented here, were performed using an access-free web knowledge base on low-energy nuclear physics (NRV) [28].

One of the main shortcomings of the ECC model is the choice of the empirical distribution function of the dynamic barrier heights [30] responsible for coupling of relative motion to surface vibrations. The Gaussian approximation for this function is assumed. This simplified choice often results in visible deviation of the calculated cross sections from the data at energies close to the Coulomb barrier. Even more pronounced is the effect this has on the calculated so-called barrier distribution function ( $\sim d^2(E\sigma_{\text{fus}})/dE^2$ ). In the ECC model it is the function with one maximum (see Figs. 10(b) and 10(d) of Ref. [4]) while the experimental data usually reveal a more complicated structure. The dependence of the potential energy on the deformation parameters (required in the ECC model to calculate the nucleus-nucleus potential energy, and, finally, to determine the parameters of the empirical distribution of dynamic barrier heights function) is rather uncertain, too. The parameters of this dependence are usually taken on the basis of the liquid-drop model or/and systematic comparison with the available experimental data for the reactions similar to the one under analysis.

The mentioned difficulties related to the empirical distribution function of the dynamic barrier heights were overcome in the model developed in Ref. [37]. The model is based on the original ECC model with neutron rearrangement [3], where the barrier distribution function is extracted from the QCC calculations (CCDEF code [39]). Good agreement between the

experimental data and the calculated fusion cross sections is achieved for the  $^{32}\text{S} + ^{96}\text{Zr}$  system by including up to four neutron rearrangement channels.

In this paper, we present a new method of accounting for neutron transfer channels in the processes of sub-barrier fusion. It consists of combining the QCC approach, which consistently treats coupling to rotational and/or vibrational collective excitations, and semiclassical approximation for the neutron transfer probability. The proposed method is rather prompt compared to the fully microscopical ones. It naturally includes the neutron transfer channels into the QCC computational scheme, while the problems connected with the use of the empirical distribution function of dynamic barrier heights (the crucial ingredient of the ECC approach) are avoided. We describe the method in detail in Sec. II. A few examples of the calculated cross sections and the barrier distribution functions compared with the available experimental data are given in Sec. III.

## II. MODEL

The fusion cross sections can be decomposed over partial waves and written as

$$\sigma_{\text{fus}}(E) = \frac{\pi \hbar^2}{2\mu E} \sum_{l=0}^{\infty} (2l+1) T_l(E), \quad (1)$$

where  $E$  is the center-of-mass energy,  $\mu$  is the reduced mass of the system,  $l$  is the orbital angular momentum, and  $T_l(E)$  is the barrier penetration probability. In order to find the coefficients  $T_l(E)$  using the QCC approach, one should consider the following Hamiltonian:

$$\hat{H} = -\frac{\hbar^2}{2\mu} \nabla^2 + V(r, \alpha) + \hat{H}_{\text{int}}(\alpha). \quad (2)$$

Here  $\hat{H}_{\text{int}}$  is the Hamiltonian of the internal (collective and single-particle) degrees of freedom  $\alpha$  and  $V$  is the interaction potential energy of the colliding nuclei. Then the stationary Schrödinger equation for the wave function  $\Psi_{\vec{k}}$  completed with the corresponding boundary conditions (see below) should be solved. In the no-Coriolis approximation, often referred to as the isocentrifugal approximation [25], the total wave function can be decomposed over the partial waves as

$$\Psi_{\vec{k}}(r, \theta; \alpha) = \frac{1}{kr} \sum_{l=0}^{\infty} i^l e^{i\sigma_l} (2l+1) \chi_l(r, \alpha) P_l(\cos \theta), \quad (3)$$

where the definition of the Coulomb phase shifts  $\sigma_l$  is given below Eq. (10).

The set of the coupled equations for  $\chi_l(r, \alpha)$  looks to be

$$\begin{aligned} \frac{\partial^2}{\partial r^2} \chi_l(r, \alpha) - \frac{l(l+1)}{r^2} \chi_l(r, \alpha) \\ + \frac{2\mu}{\hbar^2} [E - V(r, \alpha) - H_{\text{int}}(\alpha)] \chi_l(r, \alpha) = 0. \end{aligned} \quad (4)$$

The functions  $\chi_l(r, \alpha)$  can be decomposed over a complete set of wave functions of the intrinsic motion  $\varphi_\nu(\alpha)$ , which obey

$$H_{\text{int}} \varphi_\nu(\alpha) = \varepsilon_\nu \varphi_\nu(\alpha):$$

$$\chi_l(r, \alpha) = \sum_\nu \psi_{l,\nu}(r) \varphi_\nu(\alpha), \quad (5)$$

and the radial wave functions  $\psi_{l,\nu}$  satisfy the CC differential equations [25,27]

$$\begin{aligned} \frac{\partial^2}{\partial r^2} \psi_{l,\nu}(r) - \frac{l(l+1)}{r^2} \psi_{l,\nu}(r) + \frac{2\mu}{\hbar^2} [E - \varepsilon_\nu - V_{\nu\nu}(r)] \psi_{l,\nu}(r) \\ - \frac{2\mu}{\hbar^2} \sum_{\nu' \neq \nu} V_{\nu'\nu}(r) \psi_{l,\nu'}(r) = 0. \end{aligned} \quad (6)$$

In Eqs. (6) the coupling matrix elements  $V_{\gamma\nu}$  are given as

$$V_{\gamma\nu}(r) = \int \varphi_\nu^*(\alpha) V(r, \alpha) \varphi_\nu(\alpha) d\alpha. \quad (7)$$

At this point the internal degrees of freedom  $\alpha$  and the corresponding total potential energy of the system should be defined. It is well known that the standard QCC model takes into account only collective degrees of freedom (deformations  $\beta_{i\lambda}$  of multipolarity  $\lambda = 2, 3, \dots$  and/or angles of mutual orientations  $\theta_i$  of colliding nuclei,  $i = 1, 2$ ). The potential energy of two deformable and/or rotating nuclei  $V(r, \alpha)$  is a sum of the Coulomb and nuclear energies

$$V(r, \alpha) = V_C(r, \alpha) + V_N(r, \alpha). \quad (8)$$

The internal Hamiltonian  $H_{\text{int}}(\alpha)$  has a form

$$H_{\text{int}}(\alpha) = \sum_{i=1,2} \frac{\hbar^2 \hat{I}_i^2}{2\mathfrak{J}_i} + \sum_{i=1,2} \sum_{\lambda \geq 2} \left( -\frac{1}{2d_{i\lambda}} \frac{\partial^2}{\partial \beta_{i\lambda}^2} + \frac{1}{2} C_{i\lambda} \beta_{i\lambda}^2 \right), \quad (9)$$

where  $\mathfrak{J}_i$  are the moments of inertia of the colliding nuclei,  $C_{i\lambda}$  are the rigidities to the deformation of multipolarity  $\lambda$ , and  $d_{i\lambda}$  are the inertia parameters of surface vibrations.

The CC equations (6) are completed with the boundary conditions as follows. Not so heavy nuclei, colliding at near-barrier energies, are assumed to fuse (i.e., form a compound nucleus) with the probability close to unity, once they overcome the Coulomb barrier and come into contact. In that case the fusion cross section can be measured by detecting all the fission fragments and evaporation residues. Thus when formulating the boundary conditions for the wave function  $\Psi_{\vec{k}}(r, \theta; \alpha)$ , the flux that overcomes the Coulomb barrier is usually assumed to be absorbed completely (and form a compound nucleus) and not to be reflected from the inner region. This means that at  $r < R_{\text{fus}} \approx R_1 + R_2$  the functions  $\chi_l(r, \alpha)$  are the incoming waves, and there are no outgoing components reflected from the region  $0 \leq r \leq R_{\text{fus}}$  [27]. At larger distances, ( $r \rightarrow \infty$ ) the wave function behaves as a scattering wave: the incoming and outgoing waves in the elastic channel,  $\nu = 0$ , and the outgoing waves in the rest of the channels. For the partial wave functions, this corresponds to the condition

$$\begin{aligned} \psi_{l,\nu}(r \rightarrow \infty) \\ = \frac{i}{2} \left[ h_l^{(-)}(\eta_\nu, k_\nu r) \delta_{\nu 0} - \left( \frac{k_0}{k_\nu} \right)^{1/2} S_{\nu 0} h_l^{(+)}(\eta_\nu, k_\nu r) \right], \end{aligned} \quad (10)$$

where  $k_v^2 = \frac{2\mu}{\hbar^2} E_v$ ,  $E_v = E - \varepsilon_v$ ,  $\varepsilon_v$  is the nucleus excitation energy in the channel  $v$ , and  $\eta_v = \frac{k_v Z_1 Z_2 e^2}{2E_v}$  is the Sommerfeld parameter. The quantities  $h_l^{(\pm)}(\eta_v, k_v, r)$  are the Coulomb partial wave functions with the asymptotic behavior  $\exp(\pm i x_{l,v})$ , where  $x_{l,v} = k_v r - \eta_v \ln 2k_v r + \sigma_{l,v} - l\pi/2$ ,  $\sigma_{l,v} = \arg \Gamma(l + 1 + i\eta_v)$  are the Coulomb partial phase shifts, and  $S_{l,v}^{\pm}$  are the partial scattering matrix elements. A similar expression is obtained for the closed channels ( $E_v < 0$ ) with an imaginary argument of the function  $h_l^{(\pm)}$ . Equations (6) with these boundary conditions are solved numerically [27]. The partial penetration probability, which takes account of the effect of the vibrational and/or rotational couplings, is defined by the ratio of the passed and incoming fluxes

$$T_l^{\text{CC}}(E) = \frac{1}{j_0(E)} \sum_v j_{l,v}(E), \quad (11)$$

where  $j_{l,v} = -i \frac{\hbar}{2\mu} (\psi_{l,v} \frac{d\psi_{l,v}^*}{dr} - \psi_{l,v}^* \frac{d\psi_{l,v}}{dr})|_{r \leq R_{\text{fus}}}$  is the partial flux in the channel  $v$  and  $j_0 = \hbar k_0/\mu$ .

Let us now include neutron transfer channels into the above-described standard QCC approach. As was already mentioned, when the colliding nuclei approach each other, the neutron(s) wave function(s) can be rearranged between both nuclei already before passing through the Coulomb barrier. If the energy of the ground-state-to-ground-state transition is positive, then the neutron rearrangement may go with positive as well as with negative  $Q$  values depending on the energy of the intermediate state. In this case the kinetic energy of relative motion changes to  $E + Q$ . At positive  $Q$  values this leads to a gain in the kinetic energy and, thus, to an increase of tunneling probability through the barrier at sub-barrier energies. Such a mechanism can be phenomenologically added to the QCC approach. The incoming flux can penetrate the multidimensional Coulomb barrier in different neutron rearrangement channels with the probability  $\alpha_x(E, l, Q)$  for transfer of  $x$  neutrons. In that case, the total penetration probability in Eq. (1) (which takes into account the rearrangement of neutrons) can be obtained by averaging over different neutron-transfer channels and  $Q$  values for neutron transfer:

$$T_l(E) = N_{tr}^{-1} \int_{-E}^{\max\{Q_{xn}\}} [\delta(Q) + \alpha_{tr}(E, l, Q)] \times T_l^{\text{CC}}(E + Q) dQ, \quad (12)$$

where the first term in square brackets corresponds to the no-transfer channel,  $Q_{xn}$  is the  $Q$  value of the ground-to-ground transfer of  $x$  neutrons, and the neutron transfer probability is defined as

$$\alpha_{tr}(E, l, Q) = \sum_{x=1}^{x_{\text{max}}} \alpha_x(E, l, Q), \quad (13)$$

where  $x_{\text{max}}$  is the maximal number of the included neutron transfer channels (four in the present calculations).

The standard QCC model (without neutron rearrangement) corresponds to the case of  $\alpha_{tr} = 0$  in Eq. (12), i.e., when the  $Q$ -value distribution is the  $\delta$  function and  $N_{tr} = 1$ . Consideration of coupling to neutron transfer channels leads to  $Q$  distribution, which has the typical shape shown in Fig. 1. Each  $Q_{xn}$  value

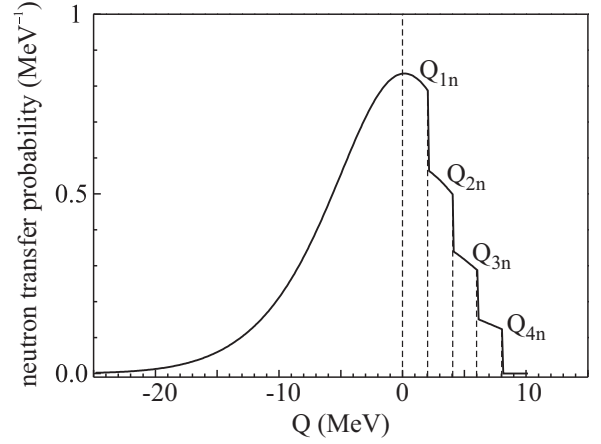


FIG. 1. Typical behavior of neutron transfer probability function  $\alpha_{tr}$  entering Eq. (12). The  $Q_{xn}$  values are assumed to be equal to  $2x$  (MeV).

gives a threshold for transfer of the corresponding number of neutrons that results in a step behavior of the  $\alpha_{tr}$  function.

The normalization constant in Eq. (12) is defined as

$$N_{tr} = 1 + \int_{-E}^{Q_{xn}} \alpha_{tr}(E, l, Q) dQ, \quad (14)$$

and the probability of transfer of  $x$  neutrons with a given  $Q$  value (less than  $Q_{xn}$ ) can be estimated semiclassically [3,40,41]:

$$\alpha_x(E, l, Q) = N_x^{-1} \exp(-Q^2/2\sigma_x^2) \times \exp(-2\kappa_x[D(E, l) - D_0]). \quad (15)$$

Note that  $N_{tr}$  is close to unity at sub-barrier energies, when the influence of neutron rearrangement channels on the fusion cross section can be visible and the semiclassical approximation is applicable. This is due to rather small values of the neutron transfer probabilities in this region (see, e.g., the results of the TDHF calculations [7] and experimental data for the  $1n - 4n$  transfer probabilities for the  $^{40}\text{Ca} + ^{96}\text{Zr}$  system [42]). Although the values of neutron transfer probabilities are small, the corresponding term in Eq. (12) is very important for deep sub-barrier energies, where the penetration probability through the fusion barrier is extremely energy sensitive.

The normalization factor  $N_x$  in Eq. (15) is defined as

$$N_x = \int_{-E}^{Q_{xn}} \exp(-Q^2/2\sigma_x^2) dQ, \quad (16)$$

and for sequential transfer of  $x$  neutrons, one has

$$\kappa_x = \sum_{i=1}^x \kappa(\varepsilon_i), \quad \kappa(\varepsilon_i) = \sqrt{2\mu_n \varepsilon_i / \hbar^2}, \quad (17)$$

where  $\varepsilon_i$  is the binding energy of the  $i$ th transferred neutron and  $\mu_n$  is the neutron reduced mass.  $D(E, l)$  is the distance of the closest approach along the Coulomb trajectory with the angular momentum  $l$ ,  $D_0 = R_1^{(n)} + R_2^{(n)} + d_0$ ,  $R_i^{(n)} = r_0^{(n)} A^{1/3}$  are the orbit radii of valence (transferred) neutrons of the colliding

nuclei ( $r_0^{(n)}$  and  $d_0$  are the adjustable parameters). The variance of the  $Q$  distribution of the neutron-transfer probability (15) is defined as [41]

$$\sigma_x = \sqrt{\frac{2\hbar^2 \kappa_x B}{\mu R_B}}, \quad (18)$$

where  $R_B$  is the barrier radius and  $B$  is the barrier height for spherical nuclei. The values of  $r_0^{(n)} = 1.25$  fm and  $d_0 = 2.5$  fm were obtained in our previous paper [4]. Note that the values  $r_0^{(n)} = 1.4$  fm and  $d_0 = 0$  were extracted [40,42,43] from the analysis of the data on transfer reactions. This leads to smaller values of  $\alpha_k$  for transfer reactions as compared to those required for fusion reactions. This difference can be understood this way: For the fusion reactions the effect from the neutron rearrangement depends on how strongly the wave function of the valence neutron is spread over the two-center molecular states at the moment of the closest approach. However, the transfer probability is given by the situation after reseparation of the colliding nuclei at infinite distances between them. Due to a certain adiabaticity of the process, transfer (rearrangement) probability should be higher at the turning point and, thus, greater in the analysis of fusion reactions.

It should be mentioned that integration over negative  $Q$  values has a rather small input to integral (12) due to a fast decrease of the barrier penetration probability  $T_l^{\text{CC}}$  at sub-barrier energies. Therefore, for practical application of the developed model, we substitute the lower limit by  $-\max\{Q_{xn}\}$ .

Note once more that the model described above is not a fully microscopical one, since it combines a quantum description of coupling of relative motion to collective degrees of freedom (surface vibrations and/or rotations) and semiclassical approximation for neutron transfer probabilities. It was mentioned above that the TDHF theory can be effectively used for analysis of processes of low-energy nucleus-nucleus collisions [7–9]. The cross sections of the few-nucleon transfer reactions calculated within the TDHF approach and within the Langevin-type model [employing the semiclassical approximation of nucleon transfer probability analogous to Eq. (15)] are in a good agreement with each other as well as with the experimental data (see Figs. 26 and 27 of Ref. [8]). A similar conclusion about the applicability of the semiclassical approximation for analysis of few-nucleon transfer reactions was made earlier in Ref. [3]. Application of the TDHF approach and the models based on the time-dependent Schrödinger equation [11,12] for nucleon transfer processes is still rather limited, in particular, since such the calculations are very time-consuming and require substantial computational resources. Therefore, the corresponding efficient semiclassical approximations are still of great value for practical use. As opposed to the fully microscopical models, they may miss some fine effects. Nevertheless, they do correctly catch the main physical regularities of the processes under analysis.

### III. TEST OF THE MODEL AND CONCLUSIONS

In this section we are going to test the proposed model. We will subsequently call it QCC+ENR (empirical neutron

TABLE I. The vibrational properties of nuclei used in our QCC calculations. The parameter  $n_{ph}$  is the number of included phonons. The data are taken from Refs. [28,45,46].

| Nucleus           | $(\lambda^\pi)^{n_{ph}}$ | $E_\lambda$ (MeV) | $\beta_\lambda$ |
|-------------------|--------------------------|-------------------|-----------------|
| $^{40}\text{Ca}$  | $(3-)^1$                 | 3.737             | 0.411           |
| $^{32}\text{S}$   | $(2+)^1$                 | 2.230             | 0.315           |
|                   | $(3-)^1$                 | 5.006             | 0.4             |
| $^{90}\text{Zr}$  | $(2+)^2$                 | 2.186             | 0.089           |
|                   | $(3-)^2$                 | 2.748             | 0.211           |
| $^{94}\text{Zr}$  | $(2+)^2$                 | 0.919             | 0.09            |
|                   | $(3-)^2$                 | 2.058             | 0.193           |
| $^{96}\text{Zr}$  | $(2+)^2$                 | 1.751             | 0.08            |
|                   | $(3-)^2$                 | 1.897             | 0.284           |
| $^{60}\text{Ni}$  | $(2+)^2$                 | 1.333             | 0.207           |
|                   | $(3-)^1$                 | 4.04              | 0.209           |
| $^{64}\text{Ni}$  | $(2+)^2$                 | 1.346             | 0.179           |
|                   | $(3-)^1$                 | 3.56              | 0.201           |
| $^{100}\text{Mo}$ | $(2+)^2$                 | 0.536             | 0.231           |
|                   | $(3-)^2$                 | 1.908             | 0.218           |

rearrangement). Note that all the considered examples below correspond to fusion of nuclei that are spherical in their ground states. Thus coupling to vibrational states is taken into account; i.e., the rotational term of the Hamiltonian (9) is lacking. However, the method can be equally applied to the systems of nuclei deformed in their ground states as well as to the deformed and spherical combinations. All the calculations were performed assuming the nuclear part of the nucleus-nucleus potential of the Woods-Saxon form with the parameters taken from the Akyüz-Winther parametrization [44]. The vibrational properties of fusing nuclei are shown in Table I. For each combination, the quadrupole and octupole vibration modes of both nuclei are considered, except for a rather weak quadrupole mode of  $^{40}\text{Ca}$  ( $E_{2+} = 3.9$  MeV,  $\beta_{2+} = 0.123$ ) neglected here. Its inclusion results in an insignificant increase of the sub-barrier fusion cross section and can be easily compensated by a small variation of the potential parameters. The  $Q$  values for the ground-state-to-ground-state neutron transfer are given in Table II. This table contains as well the values of the variances of  $Q$  distributions for transfer of  $x$  neutrons (for positive  $Q_{xn}$  values). One can see that  $\sigma_x \gtrsim Q_{xn}$  for all the cases. This results in broad  $Q$  distributions with substantial probability of neutron transfer even to the ground state of the recipient nucleus.

The first classical example of the fusion of  $^{40}\text{Ca}$  with three zirconium isotopes is shown in Fig. 2. One may notice a good agreement with the data on the fusion cross section for all three shown combinations. The neutron transfer channels are taken into consideration for the  $^{40}\text{Ca} + ^{94,96}\text{Zr}$  systems, while the data for the  $^{40}\text{Ca} + ^{90}\text{Zr}$  reaction can be reproduced taking account of coupling to vibrational states only (since all the  $Q_{xn}$  values are negative). A similar situation is observed (see Fig. 3) for the recently studied fusion reactions of  $^{32}\text{S}$  with the same three zirconium isotopes [37,49]. With regard to the previous case, there are positive  $Q_{xn}$  values for the  $^{32}\text{S} + ^{94,96}\text{Zr}$  combinations, while all  $Q_{xn}$  are negative for  $^{32}\text{S} + ^{90}\text{Zr}$  one. In spite of the overall good agreement with the data, one

TABLE II.  $Q_{xn}$  values for the ground-to-ground neutron transfer and the variances  $\sigma_x$ . The quantities are given in MeV.

| Reaction                           | $Q_{1n}$ | $\sigma_1$ | $Q_{2n}$ | $\sigma_2$ | $Q_{3n}$ | $\sigma_3$ | $Q_{4n}$ | $\sigma_4$ |
|------------------------------------|----------|------------|----------|------------|----------|------------|----------|------------|
| $^{40}\text{Ca} + ^{90}\text{Zr}$  | -3.606   |            | -1.444   |            | -5.865   |            | -4.183   |            |
| $^{40}\text{Ca} + ^{94}\text{Zr}$  | +0.143   | 4.20       | +4.890   | 5.79       | +4.188   | 7.19       | +8.125   | 8.26       |
| $^{40}\text{Ca} + ^{96}\text{Zr}$  | +0.508   | 4.13       | +5.527   | 5.69       | +5.241   | 7.06       | +9.637   | 8.10       |
| $^{32}\text{S} + ^{90}\text{Zr}$   | -3.327   |            | -1.229   |            | -6.596   |            | -6.156   |            |
| $^{32}\text{S} + ^{94}\text{Zr}$   | +0.422   | 4.18       | +5.105   | 5.75       | +3.456   | 7.15       | +6.151   | 8.21       |
| $^{32}\text{S} + ^{96}\text{Zr}$   | +0.787   | 4.10       | +5.742   | 5.65       | +4.509   | 7.02       | +7.664   | 8.05       |
| $^{64}\text{Ni} + ^{100}\text{Mo}$ | -2.194   |            | +0.833   | 5.48       | -2.002   |            | -1.031   |            |
| $^{60}\text{Ni} + ^{100}\text{Mo}$ | -0.472   |            | +4.199   | 5.65       | +2.394   | 7.04       | +5.230   | 8.08       |

may notice an insignificant overestimation of the experimental cross section for the  $^{32}\text{S} + ^{96}\text{Zr}$  reaction at deep sub-barrier region and some underestimation for the  $^{32}\text{S} + ^{94}\text{Zr}$  case. Note

that a similar underestimation is obtained for the  $^{40}\text{Ca} + ^{94}\text{Zr}$  system. This difference can be easily removed, for example, by small variation of the parameters of the nucleus-nucleus

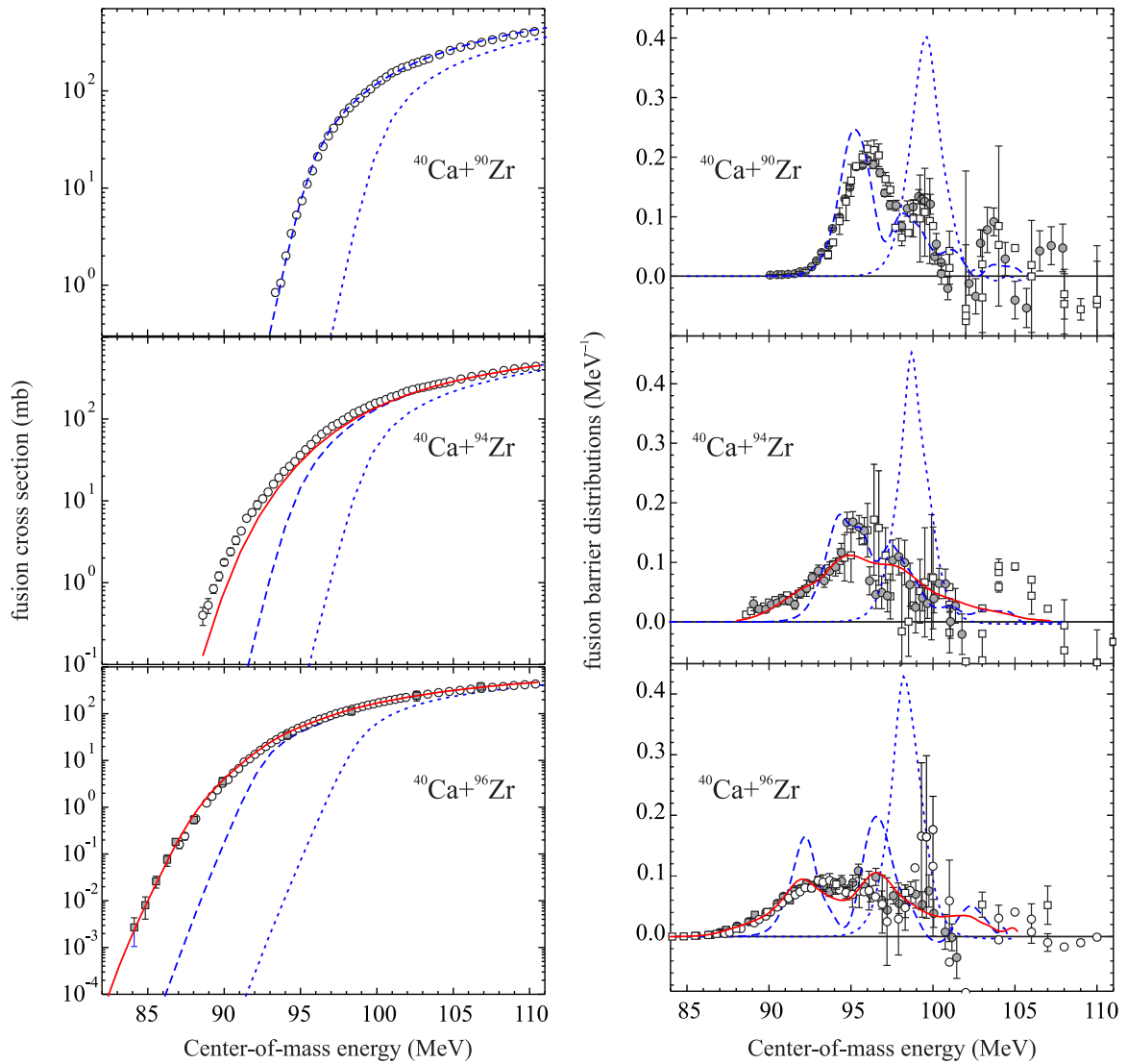


FIG. 2. (Color online) Fusion cross sections and barrier distribution functions for  $^{40}\text{Ca} + ^{90,94,96}\text{Zr}$ . The dotted curves show the no-coupling limit. The solid and dashed curves correspond to the calculations with (QCC+ENR model) and without (QCC model) taking account of neutron transfer, respectively. (Left) The experimental data on fusion cross sections are from Refs. [1] (open circles) and [47] (filled rectangles). (Right) The filled symbols are the experimental estimation of the barrier distribution functions taken from Ref. [48]. The open symbols show estimations of the same quantity made by the method proposed in Ref. [33] (see the text).

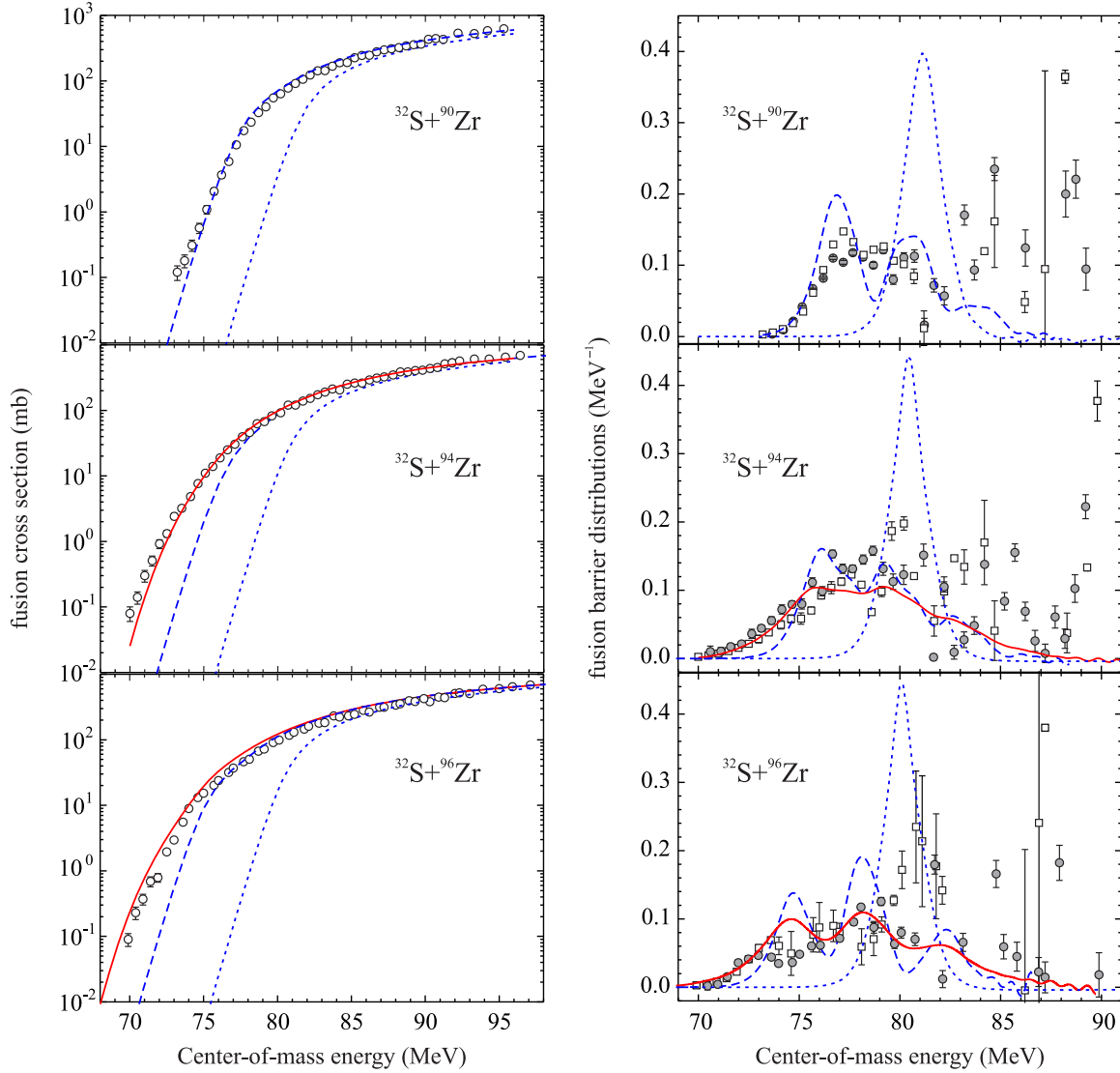


FIG. 3. (Color online) Fusion cross sections and barrier distribution functions for  $^{32}\text{S} + ^{90,94,96}\text{Zr}$ . The notations are the same as in Fig. 2. The experimental data for the fusion cross sections are taken from Ref. [37] for  $^{32}\text{S} + ^{90,96}\text{Zr}$  and from Ref. [49] for  $^{32}\text{S} + ^{94}\text{Zr}$ .

potential or the neutron radius parameters  $r_n^{(0)}$ . In this work, however, we do not fit the model parameters to the data in order to show the model's predictive power.

Furthermore, Figs. 2 and 3 show the barrier distribution functions  $D(E) = (\pi R_B^2)^{-1} d^2(E\sigma_{\text{fus}})/dE^2$ , where  $R_B$  is the barrier radius. The figures contain two sets of experimental data. One of them (filled symbols) is taken from the original experimental papers, and another one (open symbols) was obtained in our analysis using the method proposed in Ref. [33] and described in the Appendix A. We used this new method based on the spline approximation technic because the standard method described, for example, in Ref. [50], causes difficulties in performing direct double differentiation of the experimental fusion cross section. The digitized experimental data of the fusion cross section (used here) are taken from the NRV knowledge base [28]. They may contain some additional uncertainties caused by the procedure of digitizing the original experimental papers. These uncertainties, being insignificant

(and invisible) when one is discussing the fusion cross section, may result, however, in large uncertainties for the second derivative calculated by a standard finite difference method. The method described in Ref. [33] eliminates all such the uncertainties and results in a very similar barrier distributions at sub-barrier and near-barrier energy regions as compared with those taken from original experimental works.

As usual, the barrier distribution functions calculated in the single-barrier penetration model (without regard for channel coupling) are the functions with a single maximum at the barrier position (dotted curves). Consideration of coupling to the collective vibrational degrees of freedom (dashed curves) results in broadening of the barrier distributions, their shift towards lower energies, and a well-distinguished structure (few maxima). This is already sufficient for the fusion reactions with <sup>90</sup>Zr (for which neutron transfer channels do not play a role) to satisfactory agree with the experimental data in a whole energy range. For the reactions with the <sup>94,96</sup>Zr

targets, neutron rearrangement significantly influences the sub-barrier fusion, and the barrier distributions calculated without taking account of this effect are still too narrow. The solid curves are obtained within the QCC + ENR model, i.e., with neutron rearrangement. This leads to further broadening of the calculated barrier distribution functions, without their structures (number of maxima and their positions) being visibly changed. One can see overall good agreement of the calculated barrier distributions with the experimental data. This is especially relevant to the low-energy tails, which cannot be reproduced in the QCC calculations.

As mentioned above, it was concluded in our previous work [4] that the sub-barrier fusion enhancements owing to neutron rearrangement and excitation of the collective vibrational and/or rotational states are not additive. This means that neutron rearrangement channels play a significant role when the system reveals a moderate effect from coupling to the collective states. That is the case of fusion of spherical rigid (usually magic or nearly magic) nuclei, such as calcium and zirconium. If, however, one or both fusing nuclei are rather soft with respect to their deformation, then the sub-barrier fusion enhancement due to neutron rearrangement becomes less visible even in the presence of large  $Q_{xn}$  values. A good example of such kind is a pair of the  $^{60,64}\text{Ni} + ^{100}\text{Mo}$  fusion reactions studied experimentally in Refs. [51,52]. Figure 4 demonstrates a good agreement between the QCC+ENR

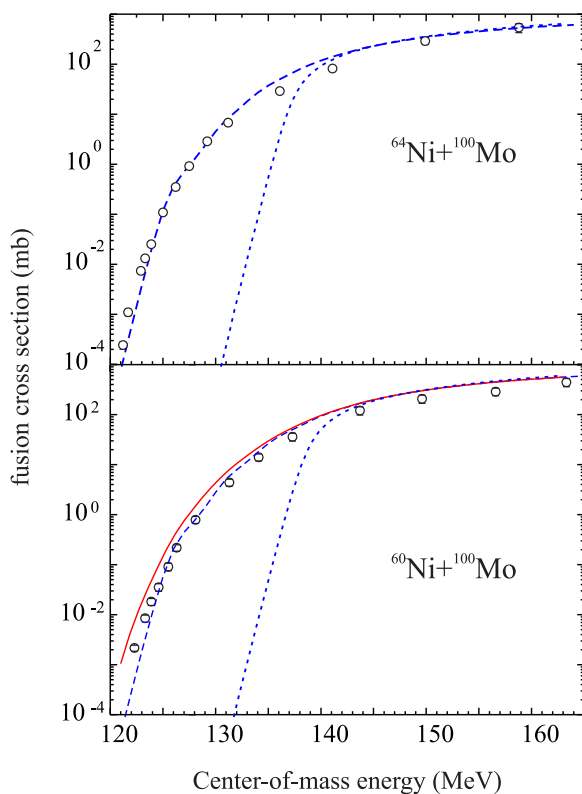


FIG. 4. (Color online) Fusion cross sections for  $^{64,60}\text{Ni} + ^{100}\text{Mo}$ . The dotted curves demonstrate the no-coupling limits. The calculations with (solid curve) and without (dashed curves) considering neutron rearrangement are shown. The experimental data are taken from Ref. [51] ( $^{64}\text{Ni} + ^{100}\text{Mo}$ ) and Ref. [52] ( $^{60}\text{Ni} + ^{100}\text{Mo}$ ).

calculations and these data as well. The  $Q_{xn}$  values for  $^{64}\text{Ni} + ^{100}\text{Mo}$  are negative while they are positive for the  $^{60}\text{Ni} + ^{100}\text{Mo}$  system and close to the  $^{40}\text{Ca} + ^{96}\text{Zr}$  combination (see Table I). However, the sub-barrier fusion cross section for the  $^{60}\text{Ni} + ^{100}\text{Mo}$  reaction differs negligibly from the  $^{64}\text{Ni} + ^{100}\text{Mo}$  case. This is attributed to softness of the  $^{100}\text{Mo}$  nucleus in comparison with a much stiffer  $^{96}\text{Zr}$ . As the result, the penetration probabilities  $T_l^{\text{CC}}$  for the Ni+Mo system decrease at sub-barrier energies much weaker than for the Ca+Zr case. Therefore, averaging over  $Q$  values in Eq. (12) has a more pronounced effect for the Ca+Zr combination. The differences between the  $Q$  values of the two reactions (and the corresponding differences between the  $\alpha_{lr}$  functions) have a much weaker effect. A more detailed discussion of the subject can be found, e.g., in Ref. [4].

To summarize, in this paper we proposed a new method of accounting for neutron transfer channels in the QCC approach. The method is based on semiclassical relations for the neutron transfer probabilities and the quantum consideration of coupling of the relative motion to the collective (vibrational and/or rotational) degrees of freedom. This new model (called QCC+ENR) was successfully tested on a few combinations of fusing nuclei. A good overall agreement with the data on the fusion cross sections as well as the barrier distribution functions was obtained without any variation of the model parameters. The QCC+ENR model confirms all the conclusions made within the empirical coupled-channel model with neutron rearrangement (see Refs. [3,4]). Furthermore, one of its advantages is a more reliable microscopic consideration of the coupling of relative motion to collective degrees of freedom since the parameters of this coupling [entering the Hamiltonian (9)] can be extracted directly from the properties of fusing nuclei. In addition, the QCC + ENR model—contrary to the ECC model—is able to reproduce the structure of the barrier distribution functions.

#### ACKNOWLEDGMENT

This work was partially supported by the Russian Foundation for Basic Research by Grant No. 15-07-07673-a.

#### APPENDIX: NUMERICAL ESTIMATION OF EXPERIMENTAL BARRIER DISTRIBUTION FUNCTION

The barrier distribution function  $D(E) = (\pi R_B^2)^{-1} \tilde{D}(E)$ , where  $\tilde{D}(E) = d^2(E\sigma_{\text{fus}})/dE^2$ , is not an experimentally measurable quantity but a result of numerical differentiation of experimental fusion cross sections. Its determination suffers a lot from the limited number of energy values as well as the experimental uncertainties of the cross section measurements. Therefore, the experimental function  $D(E)$  should be better called an estimation of the barrier distribution function since it cannot be determined unambiguously. To obtain  $D(E)$ , we use a mathematically correct procedure of two-stage spline smoothing [33]. In the initial stage the smoothing spline function  $f(E) = \ln[F(E)]$ ,  $F(E) = E\sigma_{\text{fus}}(E)$  is found



from the condition of the minimum of the functional [53]

$$\Phi_1[f(E)] = \int_{E_0}^{E_n} [f''(E)]^2 dE + \sum_{k=0}^n p_k^{-1} [f(E_k) - f_k]^2, \quad (\text{A1})$$

with the experimental values  $f_k = \ln(E_k \sigma_{\text{fus},k})$ . The values  $p_k$  give a balance between deviation from the values  $f_k$  and smoothness of the approximation and should somehow be determined. It is reasonable to assume that for the points defined with a smaller experimental uncertainty, the approximating curve should pass closer to the points (smaller  $p_k$  values), while for the points with larger relative uncertainty, the curve should be smoother (larger  $p_k$ ). Thus, we approximate  $p_k$  by the relative experimental uncertainty of the measured cross section, i.e.,

$$p_k = \frac{\Delta \sigma_{\text{fus}}}{\sigma_{\text{fus}}}. \quad (\text{A2})$$

The barrier distribution function values

$$\tilde{D}_k = F''(E_k) = g'(E_k) \exp[g(E_k)] \quad (\text{A3})$$

and estimations of their errors

$$\delta \tilde{D}_k = |g'(E_k) \exp[g(E_k)] - g'_0(E_k) \exp[g_0(E_k)]| \quad (\text{A4})$$

are calculated at the second stage by the smoothing function

$$g(E) = \ln F'(E) = f(E) + \frac{1}{2} \ln [f'(E)]^2, \quad (\text{A5})$$

which is found from the condition of the minimum of the functional analogous to Eq. (A1):

$$\Phi_2[g(E)] = \int_{E_0}^{E_n} [g''(E)]^2 dE + \sum_{k=0}^m q_k^{-1} [g(E_k) - g_k]^2. \quad (\text{A6})$$

The rough blunders are eliminated from the  $g_k$  values,  $k = 1, \dots, m$ . The value of  $g_k$  is considered as a rough blunder if it does not belong to the confidence interval for five neighboring  $g_i$  values, where  $i = k - 2, \dots, k + 2$ . The  $q_k$  values are taken as  $q_k = p_k + 0.1$ .

The function  $g_0(E)$  in Eq. (A4) is the result of calculation without smoothing, i.e., at the limit  $p_k \rightarrow 0$ .

In order to find the theoretical barrier distribution function, we use the same procedure but assume  $p_k = q_k = 0.01$ .

- 
- [1] H. Timmers, D. Ackermann, S. Beghini, L. Corradi, J. H. He, G. Montagnoli, F. Scarlassara, A. M. Stefanini, and N. Rowley, *Nucl. Phys. A* **633**, 421 (1998).
- [2] A. M. Borges, C. P. da Silva, D. Pereira, L. C. Chamon, E. S. Rossi, Jr., and C. E. Aguiar, *Phys. Rev. C* **46**, 2360 (1992).
- [3] V. I. Zagrebaev, *Phys. Rev. C* **67**, 061601 (2003).
- [4] V. A. Rachkov, A. V. Karpov, A. S. Denikin, and V. I. Zagrebaev, *Phys. Rev. C* **90**, 014614 (2014).
- [5] A. Winther, *Nucl. Phys. A* **572**, 191 (1994); **594**, 203 (1995).
- [6] E. Vigezzi and A. Winther, *Ann. Phys. (N.Y.)* **192**, 432 (1989).
- [7] A. S. Umar, V. E. Oberacker, and J. A. Maruhn, *Eur. Phys. J. A* **37**, 245 (2008).
- [8] K. Sekizawa and K. Yabana, *Phys. Rev. C* **88**, 014614 (2013).
- [9] C. Simenel, *Eur. Phys. J. A* **48**, 152 (2012).
- [10] K. Yabana, *Prog. Theor. Phys.* **97**, 437 (1997).
- [11] V. I. Zagrebaev, V. V. Samarin, and W. Greiner, *Phys. Rev. C* **75**, 035809 (2007).
- [12] V. V. Samarin, *Phys. At. Nucl.* **78**, 128 (2015); **78**, 861 (2015).
- [13] V. I. Zagrebaev and W. Greiner, *Phys. Rev. C* **87**, 034608 (2013).
- [14] V. I. Zagrebaev, B. Fornal, S. Leoni, and W. Greiner, *Phys. Rev. C* **89**, 054608 (2014).
- [15] A. S. Fomichev, I. David, Z. Dlouhy, S. M. Lukyanov, Yu. Ts. Oganessian, Yu. E. Penionzhkevich, V. P. Perehlygin, N. K. Skobelev, O. B. Tarasov, and R. Wolski, *Z. Phys. A* **351**, 129 (1995).
- [16] J. J. Kolata, V. Guimarães, D. Peterson, P. Santi, R. White-Stevens, P. A. DeYoung, G. F. Peaslee, B. Hughey, B. Atalla, M. Kern, P. L. Jolivet, J. A. Zimmerman, M. Y. Lee, F. D. Becchetti, E. F. Aguilera, E. Martínez-Quiroz, and J. D. Hinnefeld, *Phys. Rev. Lett.* **81**, 4580 (1998).
- [17] M. Trotta, J. L. Sida, N. Alamanos, A. Andreyev, F. Auger, D. L. Balabanski, C. Borcea, N. Coulier, A. Drouart, D. J. C. Durand, G. Georgiev, A. Gillibert, J. D. Hinnefeld, M. Huyse, C. Jouanne, V. Lapoux, A. Lépine, A. Lumbroso, F. Marie, A. Musumarra, G. Neyens, S. Ottini, R. Raabe, S. Ternier, P. Van Duppen, K. Vyvey, C. Volant, and R. Wolski, *Phys. Rev. Lett.* **84**, 2342 (2000).
- [18] A. Navin, V. Tripathi, Y. Blumenfeld, V. Nanal, C. Simenel, J. M. Casandjian, G. de France, R. Raabe, D. Bazin, A. Chatterjee, M. Dasgupta, S. Kailas, R. C. Lemmon, K. Mahata, R. G. Pillay, E. C. Pollacco, K. Ramachandran, M. Rejmund, A. Shrivastava, J. L. Sida, and E. Tryggestad, *Phys. Rev. C* **70**, 044601 (2004).
- [19] Yu. E. Penionzhkevich, V. I. Zagrebaev, S. M. Lukyanov, and R. Kalpakchieva, *Phys. Rev. Lett.* **96**, 162701 (2006); S. M. Lukyanov, Yu. E. Penionzhkevich, R. A. Astabatiev, N. A. Demekhina, Z. Dlouhy, M. P. Ivanov, R. Kalpakchieva, A. A. Kulko, E. R. Markarian, V. A. Maslov, R. V. Revenko, N. K. Skobelev, V. I. Smirnov, Yu. G. Sobolev, W. Trazska, and S. V. Khlebnikov, *Phys. Lett. B* **670**, 321 (2009).
- [20] N. Keeley, R. Raabe, N. Alamanos, and J. L. Sida, *Prog. Part. Nucl. Phys.* **59**, 579 (2007).
- [21] A. M. Vinodkumar, W. Loveland, P. H. Sprunger, L. Prissbrey, M. Trinczek, M. Dombosky, P. Machule, J. J. Kolata, and A. Roberts, *Phys. Rev. C* **80**, 054609 (2009).
- [22] M. Fisichella, V. Scuderi, A. Di Pietro, P. Figuera, M. Lattuada, C. Marchetta, M. Milin, A. Musumarra, M. G. Pellegriti, N. Skukan, E. Strano, D. Torresi, and M. Zadro, *J. Phys.: Conf. Ser.* **282**, 012014 (2011); V. Scuderi, A. Di Pietro, P. Figuera, M. Fisichella, F. Amorini, C. Angulo, G. Cardella, E. Casarejos, M. Lattuada, M. Milin, A. Musumarra, M. Papa, M. G. Pellegriti, R. Raabe, F. Rizzo, N. Skukan, D. Torresi, and M. Zadro, *Phys. Rev. C* **84**, 064604 (2011).
- [23] E. F. Aguilera, P. Amador-Valenzuela, E. Martínez-Quiroz, D. Lizcano, P. Rosales, H. García-Martínez, A. Gómez-Camacho, J. J. Kolata, A. Roberts, L. O. Lamm, G. Rogachev, V. Guimarães, F. D. Becchetti, A. Villano, M. Ojaruega, M. Febbraro, Y. Chen, H. Jiang, P. A. DeYoung, G. F. Peaslee, C. Guess, U. Khadka, J. Brown, J. D. Hinnefeld, L. Acosta, E. S. Rossi, Jr, J. F. P. Huiza, and T. L. Belyaeva, *Phys. Rev. Lett.* **107**, 092701 (2011).
- [24] C. H. Dasso and S. Landowne, *Comput. Phys. Commun.* **46**, 187 (1987).
- [25] K. Hagino, N. Rowley, and A. T. Kruppa, *Comput. Phys. Commun.* **123**, 143 (1999).

- [26] M. Trotta, A. M. Stefanini, L. Corradi, A. Gadea, F. Scarlassara, S. Beghini, and G. Montagnoli, *Phys. Rev. C* **65**, 011601 (2001).
- [27] V. I. Zagrebaev and V. V. Samarin, *Phys. At. Nucl.* **67**, 1462 (2004); V. V. Samarin and V. I. Zagrebaev, *Nucl. Phys. A* **734**, E9 (2004).
- [28] Fusion code and data of the NRV: <http://nrv.jinr.ru/>.
- [29] A. M. Stefanini, F. Scarlassara, S. Beghini, G. Montagnoli, R. Silvestri, M. Trotta, B. R. Behera, L. Corradi, E. Fioretto, A. Gadea, Y. W. Wu, S. Szilner, H. Q. Zhang, Z. H. Liu, M. Ruan, F. Yang, and N. Rowley, *Phys. Rev. C* **73**, 034606 (2006).
- [30] V. I. Zagrebaev, *Phys. Rev. C* **64**, 034606 (2001).
- [31] V. V. Sargsyan, G. G. Adamian, N. V. Antonenko, W. Scheid, and H. Q. Zhang, *Phys. Rev. C* **84**, 064614 (2011).
- [32] V. V. Sargsyan, G. G. Adamian, N. V. Antonenko, W. Scheid, and H. Q. Zhang, *Phys. Rev. C* **86**, 014602 (2012).
- [33] V. V. Samarin, *EPJ Web Conf.* **86**, 00039 (2015).
- [34] V. P. Zhigunov and B. N. Zachar'ev, *The Couple Channel Approach in Quantum Theory of Scattering* (Atomizdat, Moscow, 1974).
- [35] N. F. Mott and H. S. W. Massey, *The Theory of Atomic Collisions* (Clarendon Press, Oxford, 1965).
- [36] A. Adel, V. A. Rachkov, A. V. Karpov, A. S. Denikin, M. Ismail, W. M. Seif, and A. Y. Ellithi, *Nucl. Phys. A* **876**, 119 (2012).
- [37] H. Q. Zhang, C. J. Lin, F. Yang, H. M. Jia, X. X. Xu, Z. D. Wu, F. Jia, S. T. Zhang, Z. H. Liu, A. Richard, and C. Beck, *Phys. Rev. C* **82**, 054609 (2010).
- [38] A. V. Karpov, V. A. Rachkov, A. S. Denikin, and V. I. Zagrebaev, in *Proceedings of the International Symposium on Exotic Nuclei (EXON-2014)*, edited by Yu. E. Penionzhkevich and Yu. G. Sobolev (World Scientific, Singapore, 2015), p. 103.
- [39] J. Fernández-Niello, C. H. Dasso, and S. Landowne, *Comput. Phys. Commun.* **54**, 409 (1989).
- [40] W. von Oertzen, H. G. Bohlen, B. Gebauer, R. Künkel, F. Pühlhofer, and D. Scühh, *Z. Phys. A* **326**, 463 (1987).
- [41] R. A. Broglia, G. Pollarolo, and A. Winther, *Nucl. Phys. A* **361**, 307 (1981).
- [42] L. Corradi, S. Szilner, G. Pollarolo, G. Colò, P. Mason, E. Farnea, E. Fioretto, A. Gadea, F. Haas, D. Jelavić-Malenica, N. Mărginean, C. Michelagnoli, G. Montagnoli, D. Montanari, F. Scarlassara, N. Soić, A. M. Stefanini, C. A. Ur, and J. J. Valiente-Dobón, *Phys. Rev. C* **84**, 034603 (2011).
- [43] L. Corradi, G. Pollarolo, and S. Szilner, *J. Phys. G* **36**, 113101 (2009).
- [44] Ó. Akyüz and A. Winther, in *Proceedings of the International School of Physics, Enrico Fermi, Course LXXVII*, edited by R. A. Broglia, C. H. Dasso, and R. Richi (North-Holland, Amsterdam, 1981).
- [45] S. Raman, C. W. Nestor, Jr., and P. Tikkanen, *At. Data Nucl. Data Tables* **78**, 1 (2001).
- [46] T. Kibedi and R. H. Spear, *At. Data Nucl. Data Tables* **80**, 35 (2002).
- [47] A. M. Stefanini, G. Montagnoli, H. Esbensen, L. Corradi, S. Courtin, E. Fioretto, A. Goasduff, J. Grebosz, F. Haas, M. Mazzocco, C. Michelagnoli, T. Mijatović, D. Montanari, G. Pasqualato, C. Parascandolo, F. Scarlassara, E. Strano, S. Szilner, and D. Torresi, *Phys. Lett. B* **728**, 639 (2014).
- [48] A. M. Stefanini, B. R. Behera, S. Beghini, L. Corradi, E. Fioretto, A. Gadea, G. Montagnoli, N. Rowley, F. Scarlassara, S. Szilner, and M. Trotta, *Phys. Rev. C* **76**, 014610 (2007).
- [49] H. M. Jia, C. J. Lin, F. Yang, X. X. Xu, H. Q. Zhang, Z. H. Liu, Z. D. Wu, L. Yang, N. R. Ma, P. F. Bao, and L. J. Sun, *Phys. Rev. C* **89**, 064605 (2014).
- [50] M. Dasgupta, D. J. Hinde, N. Rowley, and A. M. Stefanini, *Annu. Rev. Nucl. Part. Sci.* **48**, 401 (1998).
- [51] C. L. Jiang, K. E. Rehm, H. Esbensen, R. V. F. Janssens, B. B. Back, C. N. Davids, J. P. Greene, D. J. Henderson, C. J. Lister, R. C. Pardo, T. Pennington, D. Peterson, D. Seweryniak, B. Shumard, S. Sinha, X. D. Tang, I. Tanihata, S. Zhu, P. Collon, S. Kurtz, and M. Paul, *Phys. Rev. C* **71**, 044613 (2005).
- [52] A. M. Stefanini, G. Montagnoli, F. Scarlassara, C. L. Jiang, H. Esbensen, E. Fioretto, L. Corradi, B. B. Back, C. M. Deibel, B. Di Giovine, J. P. Greene, H. D. Henderson, S. T. Marley, M. Notani, N. Patel, K. E. Rehm, D. Sewerinyak, X. D. Tang, C. Ugalde, and S. Zhu, *Eur. Phys. J. A* **49**, 63 (2013).
- [53] G. I. Marchuk, *Methods of Computational Mathematics* (Nauka, Moscow, 1980).